Journal of Pharmaceutical and Biomedical Analysis 48 (2008) 1029–1036

Contents lists available at ScienceDirect

Journal of Pharmaceutical and Biomedical Analysis

journal homepage: www.elsevier.com/locate/jpba

Short communication

Interaction of anthracycline disaccharide with human serum albumin: Investigation by fluorescence spectroscopic technique and modeling studies

Fengling Cui[a,*], Lixia Qin[a], Guisheng Zhang[a,**], Qingfeng Liu[a], Xiaojun Yao[b], Beilei Lei[b]

[a] College of Chemistry and Environmental Science, Key Laboratory for Environmental Pollution Control Technology of Henan Province, Henan Normal University, Xinxiang 453007, People's Republic of China
[b] Department of Chemistry, Lanzhou University, Lanzhou 730000, People's Republic of China

ARTICLE INFO

Article history:
Received 11 June 2008
Received in revised form 6 July 2008
Accepted 7 July 2008
Available online 18 July 2008

Keywords:
Disaccharide anthracycline (ADNR-3)
Human serum albumin (HSA)
Fluorescence quenching
Molecular modeling
Synchronous fluorescence

ABSTRACT

Anthracyclines are considered to be some of the most effective anticancer drugs for cancer therapy. However, drug resistance and cardiotoxicity of anthracyclines limit their clinical application. An 3′-azido disaccharide analogue of daunorubicin, 7-[4-*O*-(2,6-dideoxy-3-*O*-methyl-α-L-*arabino*-hexopyranosyl)-3-azido-2,3,6-trideoxy-α-L-*lyxo*-hexopyranosyl]daunorubicinone (ADNR-3), was shown to exhibit 10-fold better activity than parent compound daunorubicin against the drug-resistant cells and completely overcomes the drug resistance with same IC_{50} in both drug-resistant and drug-sensitive cells. In this paper, the interactions between ADNR-3 and human serum albumin (HSA) have been studied by spectroscopic techniques. By the analysis of fluorescence spectrum and fluorescence intensity, it was observed that the ADNR-3 has a strong ability to quench the intrinsic fluorescence of HSA through a static quenching procedure. The association constants of ADNR-3 with HSA were determined at different temperatures based on fluorescence quenching results. The negative ΔH and positive ΔS values in case of ADNR-3–HSA complexes showed that both hydrogen bonds and hydrophobic interactions play a role in the binding of ADNR-3 to HSA. Furthermore, synchronous fluorescence spectroscopy data and UV–vis absorbance spectra have suggested that the association between ADNR-3 and HSA changed the molecular conformation of HSA and the hydrophobic interactions play a major role in ADNR-3–HSA association. Moreover, the study of computational modeling indicated that ADNR-3 could bind to the site I of HSA and hydrophobic interaction was the major acting force for the second type of binding site, which was in agreement with the thermodynamic analysis. The distance, *r*, between donor (HSA) and acceptor (ADNR-3) was obtained according to the Förster's theory of non-radiation energy transfer. In addition, the effects of common ions on the binding constants of ADNR-3–HSA complexes were also investigated.

1. Introduction

Anthracyclines are considered to be some of the most effective anticancer drugs for cancer therapy. However, drug resistance and cardiotoxicity of anthracyclines limit their clinical application. To overcome drug resistance, in our previous research [1], we synthesized a novel class of disaccharide analogues of daunorubicin against drug-resistant leukemia. In these disaccharide analogues the first (inner) sugar in the carbohydrate chain is a 3-azido-2,3,6-trideoxy-L-*lyxo*-R-hexopyranose. Of all these disaccharide anthracyclines, 7-[4-*O*-(2,6-dideoxy-3-*O*-methyl-α-L-*arabino*-hexopyranosyl)-3-azido-2,3,6-trideoxy-α-L-*lyxo*-hexopyranosyl] daunorubicinone (ADNR-3, Fig. 1) emerged as the most active compound, showing at least 17-fold higher activity against drug-resistant cells than parent compound daunorubicin. The IC_{50} values of ADNR-3 in both drug-sensitive and drug-resistant cells are identical, which indicates that ADNR-3 completely overcomes drug resistance. The compound ADNR-3 is worthy of further evaluation as a new drug candidate.

Knowledge of interaction mechanisms between drugs and plasma proteins is of crucial importance for us to understand the pharmacodynamics and pharmacokinetics of a drug. Drug binding influences the distribution, excretion, metabolism, and interaction with the target tissues. Drugs are mainly transported by human serum albumin (HSA), a1-acidic glycoprotein (a1-AGP), and lipoproteins in blood. HSA is the most important drug carrier protein [2]. It has an important role in maintaining the colloidal osmotic pressure in blood. HSA also transports and distributes exogenous and endogenous molecules and metabolites such as nutrients, hormones, fatty acids and many diverse drugs [3]. HSA is

* Corresponding author. Tel.: +86 373 3326336; fax: +86 373 3326336.
** Corresponding author. Tel.: +86 373 3325250; fax: +86 373 3325250.
E-mail addresses: fenglingcui@hotmail.com (F. Cui), zgs6668@yahoo.com (G. Zhang).

0731-7085/$ – see front matter © 2008 Elsevier B.V. All rights reserved.
doi:10.1016/j.jpba.2008.07.009

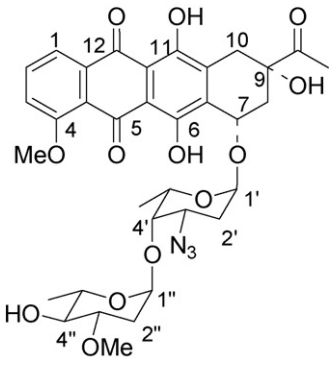

Fig. 1. The structural of ADNR-3.

a globular protein consisting of 585 amino acid residues and is considered to have three specific binding sites for high affinity binding of drugs. Each of the sites I–III, consist of two subdomains, A and B possessing common structural motifs [4,5]. Crystal structure analysis has revealed that HSA has binding sites for compounds within specialized cavities in subdomains IIA and IIIA, which correspond to site I and site II, respectively. The sole tryptophan residue (Trp-214) of HSA is in subdomain IIA [4].

The present study focused on biophysical interactions of ADNR-3 with serum albumins that play an important role in drug transport and storage in vertebrates [6]. Drug interactions at protein binding level will in most cases significantly affect the apparent distribution volume of the drugs and also affect the elimination rate of drugs. Therefore, the studies on this aspect can provide information of the structural features that determine the therapeutic effectiveness of drug, and have been an interesting research field in life sciences, chemistry and clinical medicine [7–9].

Fluorescence spectroscopy has been widely used to investigate the interaction of drug and protein. After the protein is treated by quenchers of different concentrations, quenching of the protein intrinsic fluorescence can be used to infer the binding mechanism and to calculate the number of binding site, binding constant and binding distance from the tryptophan residues [10–12]. The manner in which the fluorescence emission spectra of the bound drug–protein affected by simultaneous presence of ligands which bind specifically on the protein, leads to use the drug as a fluorescent probe to determine the environment at the drug binding site [13,14]. However, at routine experiment conditions, only tryptophan and tyrosine amino acid residues in protein can emit fluorescence, so the information relating to protein conformational changes got from fluorescence spectra must be correlative to these two residues [15–17].

The molecular interactions are often monitored by spectroscopic techniques [18], because these methods are also sensitive and relatively easy to use. They have advantages over conventional approaches such as affinity and size exclusion chromatography [19], equilibrium dialysis [20], ultrafiltration [21], and ultracentrifugation [22], which suffer from lack of sensitivity, long analysis time or both and use of protein concentrations far in excess of the dissociation constant for the drug–protein complex [23,24] and for drug–protein interaction studies. In the present paper, we are reporting the mechanism of interaction of ADNR-3 with HSA using three spectral methods for the first time.

2. Materials and methods

2.1. Materials

Appropriate amounts of HSA (Hualan Biological Engineering Limited Company) was directly dissolved in water to prepare stock solution at final concentration of 2.0×10^{-5} M and stored in the dark at 0–4 °C. 4.07×10^{-4} M ADNR-3 (synthesized), 0.5 M NaCl working solution, 0.1 M Tris–HCl buffer solution of pH 7.4 and other ionic solutions were prepared. All chemicals were of analytical reagent grade and were used without further purification. Double distilled water was used throughout.

2.2. Apparatus

All fluorescence spectra were recorded on an FP-6200 spectrofluorimeter (JASCO, Japan) and a RF-540 spectrofluorimeter (Shimadzu, Japan) equipped with a thermostat bath, using 5 nm × 5 nm slit widths. The UV absorption spectra were performed on a Tu-1810 ultraviolet-visible spectrophotometer (Beijing General Instrument, China). The pH values were measured on a pH 3 digital pH-meter (Shanghai Lei Ci Device Works, Shanghai, China) with a combined glass electrode. All calculations were performed on SGI workstation while studying the molecular model.

2.3. Synthesis and characterization of ADNR-3

ADNR-3 was synthesized starting from daunorubicin hydrochloride (Scheme 1) according to the known method [1], as a red solid in 26% total yield: HRMS $(M+Na)^+$ (ESI^+) cacld. for $C_{34}H_{39}N_3O_{13}Na^+$ 720.2375, found 720.2382. ^1H NMR (500 MHz, $CDCl_3$) 13.91 (1H, s), 13.13 (1H, s), 7.95 (1H, d, J = 7.5 Hz), 7.73 (1H, t, J = 8.2 Hz), 7.34 (1H, d, J = 8.4 Hz), 5.51 (1H, d, J = 3.4 Hz, H-1′), 5.21 (1H, d, J = 1.9 Hz, H-7), 4.93 (1H, d, J = 3.5 Hz, H-1″), 4.40 (1H, br), 4.06 (2H, m), 4.04 (3H, s), 3.70 (2H, m), 3.50 (1H, m), 3.40 (3H, s), 3.12 (2H, m), 2.83 (1H, d, J = 18.7 Hz), 2.40 (1H, m), 2.39 (3H, s), 2.24 (1H, m), 2.08 (2H, m),

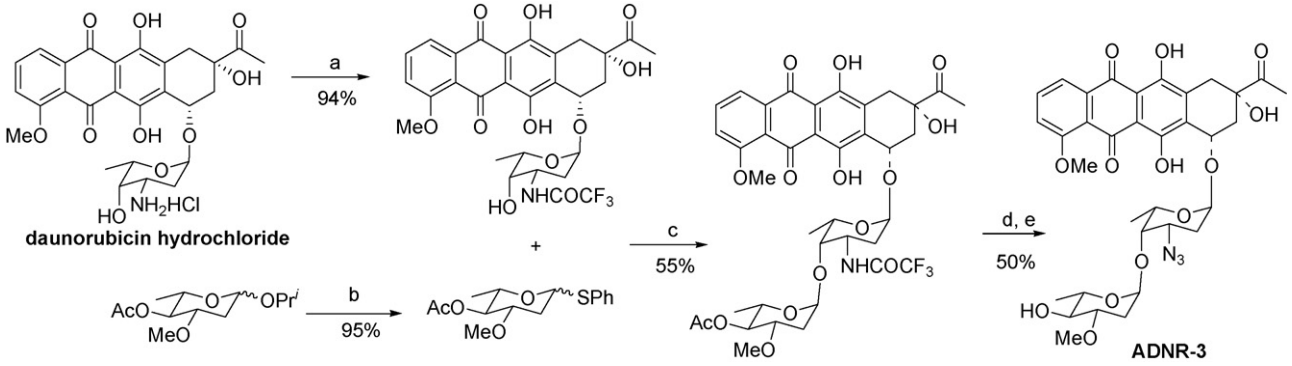

Scheme 1. Reagents and conditions: (a) $(CF_3CO)_2O$/pyridine, −20 °C, 15 min; (b) PhSH, BF_3Et_2O/CH_2Cl_2, 0 °C, 2 h; (c) TTBP, $AgPF_6/CH_2Cl_2$, 0 °C; (d) 0.1 M NaOH/THF, 0 °C; (e) K_2CO_3, $CuSO_4$,TfN_3 solution.

1.83 (1H, m), 1.52 (1H, m), 1.27 (6H, m).^{13}C NMR (125 MHz, $CDCl_3$) 211.6, 186.9, 186.6, 161.0, 156.3, 155.7, 135.7, 135.4, 134.2, 133.9, 120.8, 119.8, 118.4, 111.4, 111.3, 100.6, 99.3, 78.1, 76.7, 75.2, 69.8, 68.5, 67.9, 56.7, 56.6, 56.5, 34.9, 34.0, 33.3, 29.5, 24.7, 17.8, 17.5.

2.4. Measurements of spectrum

Under the optimum physiological conditions described above, 2.0 ml Tris–HCl buffer solution, 2.0 ml NaCl solution, appropriate amounts of HSA and ADNR-3 were added to 10.0-ml standard flask and diluted to 10.0 ml with double distilled water. Fluorescence quenching spectra of HSA were obtained at excitation wavelength (280 nm) and emission wavelength (300–450 nm). Fluorescence spectra in the presence of other ions were also measured at the same conditions. In addition, the UV absorption and synchronous fluorescence spectra of system were recorded.

2.5. Characteristics of synchronous fluorescence method

The synchronous fluorescence spectra were obtained by simultaneously scanning the excitation and emission monochromators. Thus, the synchronous fluorescence applied to the equation of synchronous luminescence [25]:

$$F = kcd\,E_{ex}(\lambda_{em} - \Delta\lambda)E_{em}(\lambda_{em}) \quad (1)$$

where F is the relative intensity of synchronous fluorescence, $\Delta\lambda = \Delta\lambda_{em} - \lambda_{ex}$ is a constant, E_{ex} the excitation function at the given excitation wavelength, E_{em} the normal emission function at the corresponding emission wavelength, c the analytical concentration, d the thickness of the sample cell, and k is the characteristic constant comprising the "instrumental geometry factor" and related parameters. Since the relationship of the synchronous fluorescence intensity (F) and the concentration of ADNR-3 should follow the F equation, F should be in direct proportion to the concentration of ADNR-3.

The optimal values of the wavelength intervals ($\Delta\lambda$) are important for the correct analysis and interpretation of the binding mechanism. When the wavelength interval ($\Delta\lambda$) was fixed at 60 nm of protein, the synchronous fluorescence had the same intensity as the emission fluorescence following excitation at 280 nm; just the emission maximum wavelength and shape of the peaks were changed [26–28]. Thus, the synchronous fluorescence measurements can be applied to calculate association constants similar to the emission fluorescence measurements. Therefore, the synchronous fluorescence measurements can deduce the binding mechanism as the emission fluorescence measurements did. In this study, the synchronous fluorescence spectra of tyrosine residues and tryptophan residues were measured at λ_{em} = 280 nm ($\Delta\lambda$ = 15 and 60 nm) in the absence and presence of various amounts of ADNR-3.

2.6. Protein-ligand docking study

The potential of the 3D structures of HSA was assigned according to the Amber 4.0 force field with Kollman-all-atom charges. The initial structures of all the molecules were generated by molecular modeling software Sybyl 6.9.1. The geometries of this drug were subsequently optimized using the Tripos force field with Gasteiger-Marsili charges. The AutoDock3.05 program was used to calculate the interaction modes between the drug and HSA. Lamarckian genetic algorithm (LGA) implemented in Autodock was applied to calculate the possible conformation of the drug that binds to the protein. During docking process, a maximum of 10 conformers was considered for the drug. The conformer with the lowest binding free energy was used for further analysis. All calculations were performed on SGI FUEL workstation.

3. Results and discussion

3.1. Analysis of HSA conformation after ADNR-3 binding

In order to obtain information about the structural perturbation of HSA, fluorescence measurements, the synchronous fluorescence and UV were performed (Figs. 2–4).

The effect of ADNR-3 on HSA and the conformation changes of HSA were evaluated by measuring the intrinsic fluorescence intensity of protein in the absence and presence of ADNR-3. Fig. 2

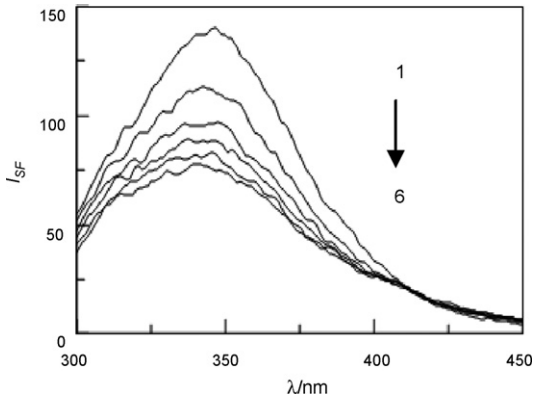

Fig. 2. The fluorescence spectra of ADNR-3–HSA system. From 1 to 6: $C_{HSA} = 2.0 \times 10^{-5}$ M; $C_{ADNR-3} = 0, 0.4, 0.8, 1.2, 1.6, 2.0 \times 10^{-5}$ M.

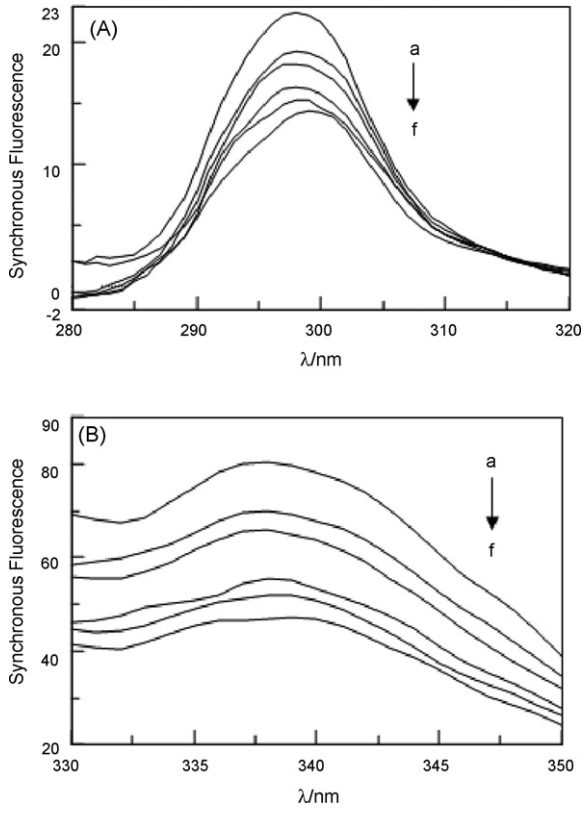

Fig. 3. Synchronous fluorescence spectrum of HSA (T = 289 K, pH 7.40), $C_{HSA} = 2 \times 10^{-5}$ M, C(ADNR-3)/(10^{-5} M), (a–f) 0, 0.4, 0.8, 1.2, 1.6, 2.0, (A) $\Delta\lambda$ = 15 nm and (B) $\Delta\lambda$ = 60 nm.

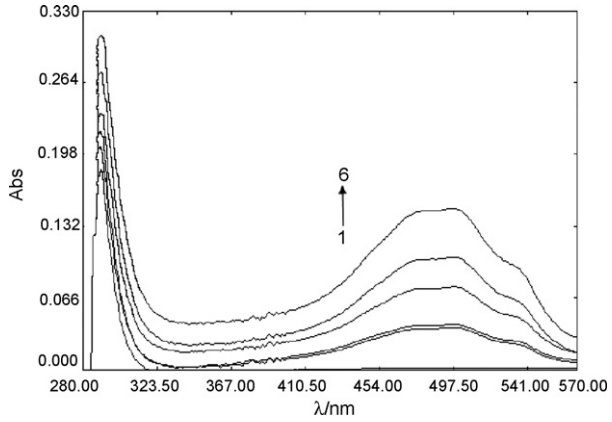

Fig. 4. UV absorption spectra of HSA in the absence and presence of ADNR-3 (1) The UV absorption of HSA, $C_{HSA} = 8 \times 10^{-7}$ M. (2) The UV absorption of ADNR-3, $C_{ADNR-3} = 4.07 \times 10^{-6}$ M. (3–6) The UV absorption of ADNR-3–HSA, $C_{HSA} = 8 \times 10^{-7}$ M; $C_{ADNR-3} = 4.07 \times 10^{-6}$ M, $C_{ADNR-3} = 8.14 \times 10^{-6}$ M, $C_{ADNR-3} = 12.21 \times 10^{-6}$ M, $C_{ADNR-3} = 16.28 \times 10^{-6}$ M.

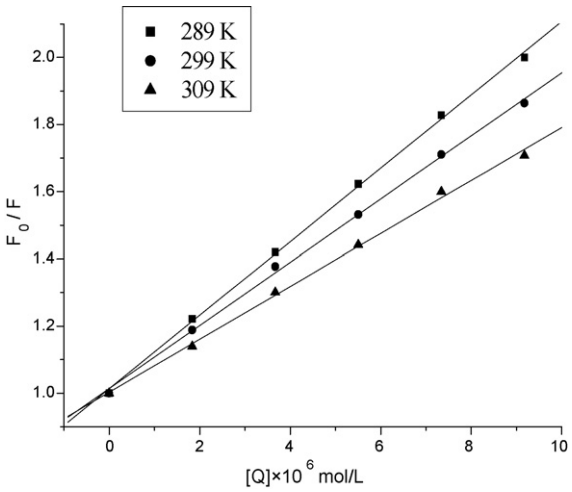

Fig. 5. The Stern–Volmer curves for quenching of ADNR-3 with HSA.

shows the fluorescence emission spectra of HSA with the addition of different concentrations of ADNR-3. HSA shows a strong fluorescence emission with a peak at 341 nm at λ_{ex} 280 nm due to its single tryptophan residue (Trp-214), while ADNR-3 was almost non-fluorescent under the present experiment conditions. It can be seen that addition of ADNR-3 to HSA leads to a significant reduction in the fluorescence intensity with a slight shift of emission to a shorter wavelength from 341 to 332 nm, indicating that the binding of ADNR-3 to HSA quenches the intrinsic fluorescence of the single tryptophan in HSA (Trp-214). It also implied that the conformational changes are induced in HSA by ADNR-3 under the conditions.

To explore the structural change of HSA by addition of ADNR-3, we measured synchronous fluorescence spectra (Fig. 3) of HSA with various amounts of ADNR-3. The synchronous fluorescence spectra give information about the molecular environment in the vicinity of the chromosphere molecules. Yuan et al. [29], suggested a useful method to study the environment of amino acid residues by measuring the possible shift in wavelength emission maximum λ_{max}, the shift in position of emission maximum corresponding to the changes of the polarity around the chromophore molecule. When the λ-value ($\Delta\lambda$) between excitation wavelength and emission wavelength was stabilized at 15 or 60 nm, the synchronous fluorescence gives the characteristic information of tyrosine residues or tryptophan residues [30]. The effect of ADNR-3 on HSA synchronous fluorescence spectroscopy is shown in Fig. 3. It is apparent from Fig. 3 that the little stronger red shift of tryptophan residues exhibits fluorescence upon addition of drug, whereas the emission maximum of tyrosine kept the position. The red shift of the emission maximum indicates that the conformation of HSA was changed and the polarity around the tryptophan residues was increased and the hydrophobicity was decreased [31].

Further experiment was carried out with UV technique to verify the binding of ADNR-3 to HSA. Fig. 4 shows the UV absorption spectra of HSA in the absence and presence of ADNR-3. As can be seen in Fig. 4, HSA has strong absorbance with a peak at 298 nm and the absorbance of HSA increased with the addition of ADNR-3; the chromophore of ADNR-3–HSA gives a very specific pattern of the UV–vis spectrum with slight dual absorbance spectra at higher concentration of ADNR-3 in the system from 472 to 540 nm. The obvious enhancement of UV absorbency intensity (A) and the change of absorption spectra verified the formation of a new complex between ADNR-3 and HSA. Thus, the evidences from fluorescence and UV spectra indicated that the interaction of ADNR-3 and HSA bring about the microenvironment change around HSA.

3.2. Quenching mechanism and binding constants

Fluorescence quenching refers to any process which decreases the fluorescence intensity of a sample. A variety of molecular interactions can result in quenching, including excited-state reactions, molecular rearrangements, energy transfer, ground-state complex formation, and collisional quenching. The different mechanisms of quenching are usually classified as either dynamic quenching or static quenching. Dynamic and static quenching can be distinguished by their differing dependence on temperature and viscosity. Dynamic quenching depends upon diffusion. Since higher temperatures result in larger diffusion coefficients, the bimolecular quenching constants are expected to increase with increasing temperature. In contrast, increased temperature is likely to result in decreased stability of complexes, and thus lower values of the static quenching constants.

In order to speculate the fluorescence quenching mechanism, the fluorescence quenching data at different temperatures (289, 299 and 309 K, Fig. 5) were firstly analyzed using the classical Stern–Volmer equation [32]:

$$\frac{F_0}{F} = 1 + k_q \tau_0 [Q] = 1 + K_{SV}[Q] \quad (2)$$

where F_0 and F are the fluorescence intensities in the absence and presence of quencher, respectively, k_q the biomolecular quenching constant, τ_0 the life time of the fluorescence in absence of quencher, [Q] the concentration of quencher, and K_{SV} is the Stern–Volmer quenching constant. The results in Table 1 show that the Stern–Volmer quenching constant K_{SV} is inversely correlated with temperature, and the values of k_q being larger than the limiting diffusion constant K_{dif} of the biomolecule ($K_{dif} = 2.0 \times 10^{10}$ M^{-1} s^{-1}) [33], which suggested that the fluorescence quenching was caused by a specific interaction between HSA and ADNR-3, and the quenching mechanism was mainly arisen from the predominant

Table 1
The dynamic quenching constants (l mol^{-1} s^{-1}) between ADNR-3 and HSA

T (K)	Stern–Volmer equation	K_q (l mol^{-1} s^{-1})	R
289	$Y = 1.0138 + 1.093 \times 10^5$ [Q]	1.093×10^{13}	0.9995
299	$Y = 1.0138 + 9.402 \times 10^4$ [Q]	9.402×10^{12}	0.9993
309	$Y = 1.0033 + 7.871 \times 10^4$ [Q]	7.871×10^{12}	0.9989

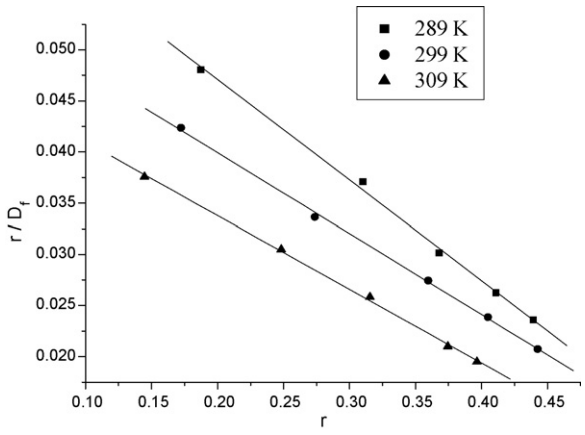

Fig. 6. Scatchard plot for the ADNR-3–HSA.

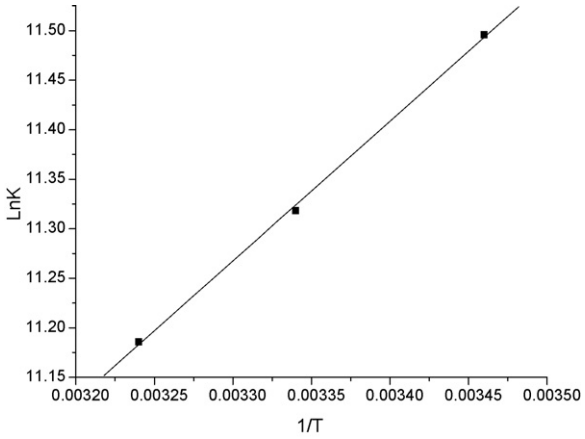

Fig. 7. Van't Hoff plot for the interaction of ADNR-3 and HSA.

of complexes formation, while dynamic collision could be negligible in the concentration studied [34]. Therefore, the quenching data were analyzed according to the Scatchard equation [35]:

$$\frac{r}{D_f} = nK - rK \tag{3}$$

where r is the number of mol of bound drug per mol of protein, D_f the concentration of unbound drug, K the binding constant, and n is the number of binding sites. Fig. 6 shows the Scatchard plots for the ADNR-3–HSA system at different temperatures. The linearity of the Scatchard plot indicated that ADNR-3 bound to a single class of binding sites on HSA, which was full agreement with the number of binding site n; and the binding constants (K, Table 2) agree very closely with those obtained by the modified Stern–Volmer equation. In addition, there was a strong interaction between ADNR-3 and HSA. The binding constant decreased with the increasing temperature, resulting in a reduction of the stability of the ADNR-3–HSA complex, but the effect of temperature is very small. Thus, the quenching efficiency of ADNR-3 to HSA is not reduced obviously when difference in temperature is not wide. In this work, the binding constants obtained by using the modified Stern–Volmer equation are applied in the discussion of binding modes.

3.3. The determination of the force acting between ADNR-3 and HSA

The interactions forces between drugs and biomolecules may include electrostatic interactions, multiple hydrogen bonds, van der Waals interactions, hydrophobic, steric contacts within the antibody-binding site, etc. In order to elucidate the interaction of ADNR-3 with HSA, the thermodynamic parameters were calculated from the van't Hoff plots.

If the enthalpy change (ΔH) does not vary significantly over the temperature range studied, then its value and that of entropy change (ΔS) can be determined from the van't Hoff equation:

$$\ln K = -\frac{\Delta H}{RT} + \frac{\Delta S}{R} \tag{4}$$

where associative binding constants K are analogous to the effective quenching constants K_a at the corresponding temperature and R is the gas constant. The temperatures used were 289, 299 and 309 K. The enthalpy change (ΔH) is calculated from the slope of the van't Hoff relationship. The free energy change (ΔG) is estimated from the following relationship:

$$\Delta G = \Delta H - T\Delta S \tag{5}$$

Fig. 7, by fitting the data of Table 3, shows that assumption of near constant ΔH is justified. Table 3 shows the values of ΔH and ΔS obtained for the binding site from the slopes and ordinates at the origin of the fitted lines. From Table 3, it can be seen that the negative sign for free energy (ΔG) means that the binding process is spontaneous. The negative enthalpy (ΔH) and positive entropy (ΔS) values of the interaction of ADNR-3 and HSA indicate that the specific hydrophobic and electrostatic interactions played major role in the reaction [36]. HSA is characterized by one tryptophan residues: Trp-214 is considered to be located within a hydrophobic pocket, which is in a well-characterized binding cavity (subdomain IIA) for small charged aromatic molecules. The crystallographic analysis of serum albumin also revealed that the major ligand binding sites are identified within this region [37], it is also known that the binding activity of the subdomain IIA affects conformational changes [38], which agrees with the conformation investigation below. Thus, combining this analysis with the structure of ADNR-3, we can infer that the binding site for ADNR-3 on HSA is mainly located in subdomain IIA. Furthermore, the specific electrostatic interactions were characterized by a concomitant increased thermal stability of the protein conformation.

3.4. Distance measurement between tryptophan and ADNR-3 binding site

Förster's theory of dipole–dipole energy transfer was used to determine the distances between the protein residue (donor) and the bound drug (acceptor) in HSA. By Förster's theory [39], the efficiency of energy transfer (E) is related to the distance R between

Table 2
The binding constant (K (M)) between ADNR-3 and HSA

T (K)	Scatchard equation	K (l/mol)	n	R
289	$Y = 0.0668 - 0.0983r$	9.83×10^4	0.6796	0.9987
299	$Y = 0.0557 - 0.0791r$	7.91×10^4	0.7047	0.9995
309	$Y = 0.0482 - 0.0721r$	7.21×10^4	0.6685	0.9994

Table 3
The thermodynamic parameters for the binding ADNR-3 to HSA

T (K)	ΔG (kJ/mol)	ΔH (kJ/mol)	ΔS (J/(mol K))
289	−27.62		
299	−28.04	−15.61	41.55
309	−28.74		

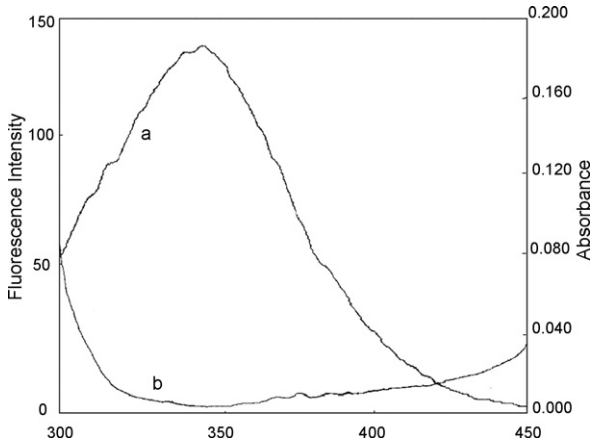

Fig. 8. The overlap of UV absorption spectrum of ADNR-3 with the fluorescence emission spectrum of HSA. (a) The fluorescence emission spectrum of HSA (8×10^{-7} M) and (b) the UV absorption spectrum of ADNR-3 (4.07×10^{-6} M).

donor and acceptor by

$$E = 1 - \frac{F}{F_0} = \frac{R_0^6}{R_0^6 + r^6} \quad (6)$$

R_0 is the distance at which the transfer efficiency equals to 50%, is given by the following equation:

$$R_0^6 = 8.8 \times 10^{-25} k^2 n^{-4} \Phi J \quad (7)$$

where n is the refractive index of the medium, K^2 the orientation factor, and Φ is the quantum yield of the donor. The spectral overlap integral (J) between the donor emission spectrum and the acceptor absorbance spectrum was approximated by the following summation:

$$J = \frac{\sum F(\lambda)\varepsilon(\lambda)\lambda^4 \ \Delta\lambda}{\sum F(\lambda)\Delta\lambda} \quad (8)$$

where $F(\lambda)$ is the fluorescence intensity of the fluorescence reagent when the wavelength is λ, $\varepsilon(\lambda)$ is the molar absorbance coefficient of the acceptor at the wavelength of λ. From these relationships J, E and R_0 can be calculated; so the value r, also can be calculated. Fig. 8 shows the overlap of the fluorescence spectra of HSA and the absorption spectra of ADNR-3. Under these experimental conditions, it has been reported for HSA that, $K^2 = 2/3$, $\Phi = 0.118$, $n = 1.336$ [40]. So the value of the overlap integral calculated from Fig. 8 is 2.072×10^{-14} cm^3 M^{-1}, and R_0 is 2.54 nm and the r is 3.1 nm, respectively. Obviously, they are lower than 7 nm after interaction between ADNR-3 and HSA. This accords with conditions of Föster's non-radioactive energy transfer theory indicated again a static quenching interaction between ADNR-3 and HSA.

3.5. Computational modeling of the ADNR-3–HSA complex

The investigation of 3D structure of crystalline albumin showed that HSA contains three homologous domains (I, II, and III): I (residues 1–195), II (196–383), and III (384–585). And each domain can be divided into two subdomains (A and B) [41]. The crystallographic analysis [4,42], has revealed that HSA has binding sites of compounds within hydrophobic cavities in subdomains IIA and IIIA, which are corresponding to site I and site II, respectively, and sole tryptophan residue (Trp-214) of HSA is in subdomain IIA. There is a large hydrophobic cavity present in subdomain IIA that many drugs can bind to.

The crystal structure of HSA in complex with warfarin was taken from the Brookhaven Protein Data Bank (entry codes 1 h9z). The potential of the 3D structure of HSA was assigned according to the Amber 4.0 force field with Kollman-all-atom charges. The initial structure of the ADNR-3 was generated by molecular modeling software Sybyl 6.9. The geometry of the molecule was subsequently optimized to minimal energy using the Tripos force field with Gasteiger-Marsili charges. Then it was used to replace warfarin in the HSA-warfarin crystal structure. At last, FlexX program was used to establish the interaction modes between the ADNR-3 and HSA. The computational modeling study was applicable to the second type of binding site in the analysis of binding reaction. It was the reason that the molar ratio of ADNR-3 to HSA of the second type of binding site was nearly 1:1. Fig. 9 exhibits the optimal energy ranked result of ADNR-3 interaction with the residues of HSA and the ADNR-3–HSA space fill conformation. It can be seen that the ADNR-3 molecule was situated within subdomain IIA hydrophobic cavity. ADNR-3 molecule moiety was located within the binding pocket and several phenyl groups of ADNR-3 were adjacent to hydrophobic residues ARG (218), TRP (214), HIS (288), etc., of subdomain IIA of HSA (site I). This fact suggested that there were hydrophobic interactions between ADNR-3 and HSA. Furthermore, there were also a number of specific electrostatic interactions and hydrogen bonds, because several ionic and polar residues in the proximity of the ligand play an important role in stabilizing the ADNR-3 molecule via H-bonds and electrostatic interaction. There were hydrogen interactions between the carbonyl group at 5-position, 6-hydroxyl group of ADNR-3 molecular and the residues LYS-195; the carbonyl group at 12-position, 11-hydroxyl group and ARG-218; the carbonyl group at 12-position, 11-hydroxyl group and ARG-222; the 11-hydroxyl group and ALA (291); 9-hydroxyl group and GLU-292 of HSA. The results suggested that the formation of hydrogen bond decreased the hydrophilicity and increased the hydrophobicity to stability in the ADNR-3–HSA system. The calculated binding Gibbs free energy (ΔG) was -22.1 kJ mol^{-1}, which was not very close to the experimental data (-27.62 kJ mol^{-1}) to some degree. A possible explanation may be that the X-ray structure of the protein from crystals differs from that of the aqueous system used in this study. Therefore, the results of modeling indicated that the interaction between ADNR-3 and HSA was dominated by hydrophobic force, which was in accord with the binding mode study. It was important to note that the Trp-214 residue of HSA was in close proximity to the drug molecule, this finding provided a good structural basis to explain the efficient fluorescence quenching of HSA emission in the presence of ADNR-3. All the proofs coming from molecular modeling illuminated that ADNR-3 could interact with HSA at site I in subdomain IIA.

3.6. Effects of other ions on binding constant of ADNR-3–HSA

The effect of common ions on the binding constant of ADNR-3–HSA system was investigated at 289 K by recording the fluorescence intensity in the range 300–450 nm upon excitation at 280 nm. The results are shown in Table 4. It is evident from the table that the binding constant between the protein and ADNR-3 increased for common ions. The higher binding constant obtained in presence of these ions might have been resulted from the interaction of cation/anion with drug to form a complex, which in turn interacted with protein. From the pharmacokinetics perspective, the increasing of the binding constant will buffer the drug concentration in the blood and prolong the duration in plasma in some way. Hence, maximum effectiveness of the drug will be achieved. Thus, the increases in binding constant of ADNR-3–HSA in presence of the above ions prolong the storage time of the drug in blood plasma and enhance the maximum effectiveness of the drug [43]. However, in case of Mg^{2+}, Ca^{2+}, Zn^{2+} and Bi^{3+} the binding constant of ADNR-3–HSA decreased resulting ADNR-3 to be quickly cleared

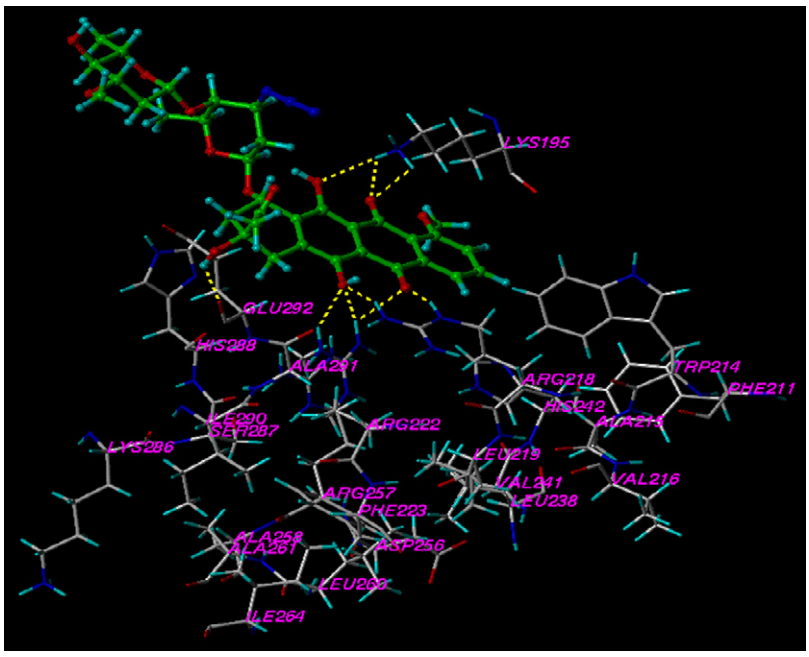

Fig. 9. The interaction model between ADNR-3 and HSA. The residues of ADNR-3 and HSA are represented using different tinctorial stick model. The hydrogen bond between the ligand and the protein is indicated by dashed line.

Table 4
The binding constants between ADNR-3 and HSA in the presence of other ions

Ions	K ($\times 10^5$)	R
Ca^{2+}	0.87	0.9993
Fe^{3+}	1.30	0.9993
F^-	1.05	0.9989
SiO_3^{2-}	1.14	0.9992
Pb^{2+}	1.21	0.9994
CO_3^{2-}	1.09	0.9993
Mg^{2+}	0.84	0.9996
SO_4^{2-}	1.08	0.9992
Ni^{2+}	1.26	0.9982
Cd^{2+}	1.32	0.9985
Bi^{3+}	0.69	0.9995
Zn^{2+}	0.86	0.9990
K^+	1.24	0.9981
Al^{3+}	1.17	0.9992
Hg^{2+}	1.44	0.9988
$C_2O_4^{2-}$	1.26	0.9997

from the blood [44], which may lead to the need for more doses of ADNR-3 to achieve the desired therapeutic effect.

4. Conclusions

This paper provided an approach for studying the interactions of fluorescent protein with ADNR-3 using absorption, fluorescence and molecular modeling techniques for the first time. We have investigated the interactions of ADNR-3 with HSA as the binding (of the drug to serum albumins) influences the drug availability at the site of action. ADNR-3 quenched the fluorescence of HSA through static quenching mechanism. This work gave a more comprehensive study and the distance between the donor (protein) and the acceptor (ADNR-3) was also calculated using FRET. The biological significance of this work is evident since albumin serves as a carrier molecule for multiple drugs and the interactions of ADNR-3 with albumin are not characterized so far. Hence, this report has a great significance in pharmacology and clinical medicine as well as methodology.

Acknowledgements

This work was sponsored by the Nature Science Foundation of China (No. 20673034), the Young Backbone Teacher Sustentation Plan of Henan Universities (No. 200470) and Department of Education of Henan Province (No. 2006150012) to F.C.; National Natural Science Foundation of China (20672031), the Program for New Century Excellent Talents in University of Henan Province (2006-HACET-06), and Innovation Scientists and Technicians Troop Construction Projects of Henan Province (084100510002) to G.Z.

References

[1] G. Zhang, L. Fang, L. Zhu, Y. Zhong, P.G. Wang, D. Sun, J. Med. Chem. 49 (2006) 1792–1799.
[2] U. Kragh-Hansen, Pharmacol. Rev. 33 (1981) 17–53.
[3] W.E. Muller, U. Wollert, Pharmacology 19 (1979) 56–59.
[4] X.M. He, D.C. Carter, Nature 358 (1992) 209–215.
[5] S. Sugio, A. Kashima, S. Mochizuki, M. Noda, K. Kobayashi, Protein Eng. Des. Sel. 12 (1999) 439–446.
[6] D. Silva, C.M. Cortez, J. Cunha-Bastos, S.R.W. Louro, Toxicol. Lett. 147 (2004) 53–61.
[7] J.Q. Liu, J.N. Tian, J.Y. Zhang, Z.D. Hu, X.G. Chen, Anal. Bioanal. Chem. 376 (2003) 864–867.
[8] K. Tang, Y.M. Qin, A.H. Lin, X. Hu, G.L. Zou, J. Pharm. Biomed. Anal. 39 (2005) 404–410.
[9] F.L. Cui, L.X. Qin, G.S. Zhang, X.J. Yao, J. Du, Int. J. Biol. Macromol. 42 (2008) 221–228.
[10] J.R. Lakowicz, Principles of Fluorescence Spectroscopy, Plenum Press, New York, 1983.
[11] M.A. Khan, S. Muzammil, J. Musarrat, Int. J. Biol. Macromol. 30 (2002) 243–249.
[12] P.B. Kandagal, S. Ashoka, J. Seetharamappa, S.M.T. Shaikh, Y. Jadegoud, O.B. Ijare, J. Pharm. Biomed. Anal. 41 (2006) 393–399.
[13] M. Otagiri, K. Masuda, T. Imai, Y. Imamura, M. Yamasaki, Biochem. Pharmacol. 38 (1989) 1–7.
[14] M.H. Rahman, T. Maruyama, T. Okada, K. Yamasaki, Biochem. Pharmacol. 46 (1993) 1721–1731.
[15] J. Shobini, A.K. Mishra, K. Sandhya, N. Chandra, Spectrochim. Acta A 57 (2001) 1133–1147.
[16] W.Y. He, Y. Li, J.N. Tian, H.X. Liu, Z.D. Hu, X.G. Chen, J. Photochem. Photobiol. A 174 (2005) 53–61.
[17] N. Seedher, S. Bhatia, Pharmcol. Res. 54 (2006) 77–84.
[18] F.L. Cui, J. Fan, J.P. Li, Z.D. Hu, Bioorg. Med. Chem. 12 (2004) 151–157.
[19] J. Szpunara, A. Makarov, T. Pieper, B.K. Keppler, R. Lobinski, Anal. Chim. Acta 387 (1999) 135–144.

[20] S.J. Zargar, A. Rabbani, Int. J. Biol. Macromol. 30 (2002) 113–117.
[21] F. Lebrun, A. Bazus, P. Dhulster, D. Guillochon, J. Membr. Sci. 146 (1998) 113–124.
[22] A.H.A. Clayton, M.A. Perugini, J. Weinstock, J. Rothacker, K.G. Watson, A.W. Burgess, E.C. Nice, Anal. Biochem. 342 (2005) 292–299.
[23] J. Oravcova, B. Bobs, W. Lindner, J. Chromatogr. B 677 (1996) 1–28.
[24] D.E. Epps, T.J. Raub, V. Caiolfa, A. Chiari, M. Zamai, J. Pharm. Pharmacol. 51 (1998) 41–48.
[25] S. Rubio, A. Gomez-Hens, M. Ualcarcel, Talanta 33 (1986) 633–640.
[26] Y.Q. Wang, H.M. Zhang, G.C. Zhang, W.H. Tao, S.H. Tang, J. Mol. Struct. 830 (2007) 40–45.
[27] Y.J. Hua, Y. Liu, J.B. Wang, X.H. Xiao, S.S. Qu, J. Pharm. Biomed. Anal. 36 (2004) 915–919.
[28] D.J. Li, J.F. Zhu, J. Jin, X.J. Yao, J. Mol. Struct. 846 (2007) 34–41.
[29] T. Yuan, A.M. Weljie, H.J. Vogel, Biochemistry 37 (1998) 3187–3195.
[30] W.C. Abert, W.M. Gregory, G.S. Allan, Anal. Biochem. 213 (1993) 407–413.
[31] B. Klajnert, M. Bryszewska, Bioelectrochemistry 55 (2002) 33–35.
[32] M.R. Eftink, Biophysical and Biochemical Aspects of Fluorescence Spectroscopy, Plenum Press, New York, 1991.
[33] J.R. Lakowica, G. Weber, Biochemistry 12 (1973) 4161–4170.
[34] M.M. Yang, X.L. Xi, P. Yang, Chin. J. Chem. 24 (2006) 642–648.
[35] G. Scatchard, I.H. Scheiberg, S.H. Armstrong, J. Am. Chem. Soc. 72 (1950) 535–540.
[36] S.N. Timaseff, in: H. Peeters (Ed.), Proteins of Biological Fluids, Pergamon Press, Oxford, 1972, pp. 511–519.
[37] D.C. Carter, X.M. He, Science 249 (1990) 302–303.
[38] P. Mi˘skovskǐy, D. Jancura, S. Sǐanchez-Cortĭes, E. Ko˘ci˘sovĭa, L. Chinsky, J. Am. Chem. Soc. 120 (1998) 6374–6379.
[39] L. Stryer, Annu. Rev. Biochem. 47 (1978) 819–846.
[40] L. Cyril, J.K. Earl, W.M. Sperry, Biochemists Handbook, E & FN Epon Led. Press, London, 1961, 83.
[41] C. Bertucci, G. Ascoli, G.U. Barretta, L.D. Bari, P. Salvadori, J. Pharm. Biomed. Anal. 13 (1995) 1087–1093.
[42] S. Curry, H. Mandelkow, P. Brick, N. Franks, Nat. Struct. Mol. Biol. 5 (1998) 827–835.
[43] F.L. Cui, J. Fan, W. Li, Y.C. Fan, Z.D. Hu, J. Pharm. Biomed. Anal. 34 (2004) 189–197.
[44] Y. Li, W. He, J. Liu, F. Sheng, Z. Hu, X. Chen, BBA-Gen. Subjects 1722 (2005) 15–21.